

Molecular BioSystems

Accepted Manuscript



This is an *Accepted Manuscript*, which has been through the Royal Society of Chemistry peer review process and has been accepted for publication.

Accepted Manuscripts are published online shortly after acceptance, before technical editing, formatting and proof reading. Using this free service, authors can make their results available to the community, in citable form, before we publish the edited article. We will replace this *Accepted Manuscript* with the edited and formatted *Advance Article* as soon as it is available.

You can find more information about *Accepted Manuscripts* in the [Information for Authors](#).

Please note that technical editing may introduce minor changes to the text and/or graphics, which may alter content. The journal's standard [Terms & Conditions](#) and the [Ethical guidelines](#) still apply. In no event shall the Royal Society of Chemistry be held responsible for any errors or omissions in this *Accepted Manuscript* or any consequences arising from the use of any information it contains.



www.rsc.org/molecularbiosystems

PAPER

Phosphorylation of Ser8 promotes zinc-induced dimerization of amyloid- β metal-binding domain†

Cite this: DOI: 10.1039/x0xx00000x

Alexandra A. Kulikova,^a Philipp O. Tsvetkov,^a Maria I. Indeykina,^{a,b} Igor A. Popov,^b Sergey S. Zhokhov,^c Andrey V. Golovin,^d Vladimir I. Polshakov,^c Evgeny Nudler,^e Sergey A. Kozin^{a,f} and Alexander A. Makarov^{*a}Received 00th June 2014,
Accepted 00th June 2014

DOI: 10.1039/x0xx00000x

www.rsc.org/

Zinc-induced aggregation of the amyloid- β peptide (A β) is a hallmark molecular feature of Alzheimer's disease (AD). Recently it was shown that phosphorylation of A β at Ser8 promotes the formation of toxic aggregates. In this work, we have studied the impact of Ser8 phosphorylation on the mode of zinc interaction with the A β metal-binding domain 1-16 using isothermal titration calorimetry, electrospray ionization mass spectrometry and NMR spectroscopy. We have discovered a novel zinc binding site (⁶HDpS⁸) in the phosphorylated peptide, in which the zinc ion is coordinated by imidazole ring of His6, phosphate group attached to Ser8 and a backbone carbonyl group of His6 or Asp7. Interaction of zinc ion with this site involves His6, thereby withdrawing it from the interaction pattern observed in the non-modified peptide. This event was found to stimulate dimerization of peptide chains through the ¹¹EVHH¹⁴ site, where the zinc ion is coordinated by the two pairs of Glu11 and His14 in the two peptide subunits. The proposed molecular mechanism of zinc-induced dimerization could contribute to the understanding of initiation of pathological A β aggregation, and the ¹¹EVHH¹⁴ tetrapeptide can be considered as a promising drug target for the prevention of amyloidogenesis.

Introduction

Alzheimer's disease (AD) is a neurodegenerative disorder, characterized by the deposition of insoluble fibrillar plaques of amyloid- β peptide (A β) and neurofibrillary tangles of hyperphosphorylated tau protein in the brain of AD patients. According to the amyloid hypothesis, the key event in the initiation of the AD pathogenesis is the aggregation of the 40-42 amino acids long soluble A β into oligomers, and subsequently into insoluble fibrils, the main component of amyloid plaques.^{1,2} Molecular mechanism of the A β aggregation remains unclear. It is known that an important role in this process is played by zinc ions,^{3,4} however their presence is not sufficient for induction of amyloidosis *in vivo*. Indeed, it was shown that even in the presence of zinc ions synthetic A β unlike A β -containing brain extracts, does not cause amyloidosis when injected intracerebrally in animal models of AD.⁵ Accordingly it was suggested that numerous post-translational modifications (PTM) of A β may serve as the pathogenic factors initiating its oligomerization.⁶⁻⁹ The plaques represent a heterogeneous mixture of different forms of A β including truncated forms,¹⁰ isomers,¹¹ racemates,⁹ piroglutamat modified⁸ and phosphorylated forms of A β .^{7,12} All these PTMs affect the conformational properties of

A β ,¹³⁻¹⁵ and may contribute to its oligomerization^{14,16,17} and cytotoxic properties.^{13,15} We have shown earlier that the isomerization of Asp7 not only enhances A β dimerization¹⁸ but leads to its increased cytotoxicity¹⁹ and also accelerates the formation of amyloid plaques in transgenic animals when administered intravenously.²⁰ Recent results from Walter's group show that phosphorylation of A β at Ser8 promotes formation of toxic aggregates.^{12,21,22} Phosphorylated A β was detected in the brains of transgenic mice and human AD brains.²¹ The mechanism of increased propensity to form toxic aggregates by A β phosphorylated at Ser8 (pA β) remains unknown. It has been suggested¹² that such propensity can be linked to the stabilization of the β -sheet conformation of pA β . Since Ser8 is located in the minimal zinc-binding site of A β , the fragment 6-14,²³ the aggregate properties of pA β may also be associated with the changes in its interactions with zinc ions. The metal-binding domain 1-16 of A β (A β (1-16)) serves as a good model for the analysis of these interactions, since it does not aggregate in aqueous solutions in the presence of zinc ions, in contrast to the full-length form of A β .^{18,23-25}

In this work, in order to investigate the impact of Ser8 phosphorylation on Zn²⁺ binding to A β , we studied Zn²⁺ interactions with the metal-binding domain of A β phosphorylated at Ser8

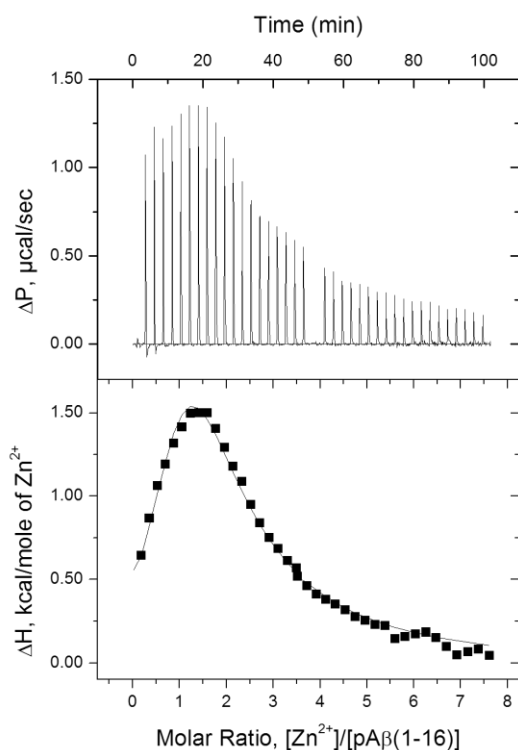


Fig. 1 ITC titration curve (upper panel) and binding isotherm (lower panel) for zinc (5 mM) interaction with pAβ(1-16) (0.3 mM) at 25°C in 20 mM Pipes buffer in the presence of 160 mM NaCl, pH 7.3.

Table 1. Thermodynamic parameters of Zn²⁺ binding to pAβ(1-16) fragments and mutants obtained by ITC at 25°C in 20 mM Pipes buffer in the presence of 160 mM NaCl, pH 7.3.

Peptide	N ^a	K _a × 10 ⁻⁴ (M ⁻¹) ^b	ΔH (kcal M ⁻¹) ^a	TΔS (kcal M ⁻¹)
Aβ(1-16) ^c	1.1	1.8	-4	1.8
	1.2	4.08	1	7.2
pAβ(1-16)	0.5	0.14	13	17.2
pAβ(1-10)	1.2	0.16	5.3	9.7
	1.2	3.3	1	7.1
pAβ(1-16)open	0.5	0.4	15	19.5
Aβ(11-16)	0.5	3.11	-0.4	6.6
pAβ(1-10)D1A	1	0.12	5.7	9.8
pAβ(1-10)E3A	1	0.16	5.9	10.1
pAβ(1-10)H6A			ND	
pAβ(1-10)D7A	1.3	0.2	4.4	8.6
pAβ(7-9)			ND	

^a Standard deviation does not exceed ±10%. ^b Standard deviation does not exceed ±20%. ^c Data from. ²³

(pAβ(1-16)). We have analyzed a set of fragments and mutants of pAβ(1-16) by isothermal titration calorimetry (ITC), NMR spectroscopy and electrospray ionization mass spectrometry (ESI-MS) in order to localize Zn²⁺ chelators. We also used quantum-mechanical/molecular-mechanical calculations (QM/MM) to model the geometry of the zinc ion chelation site.

Results

Impact of Ser8 phosphorylation on the structure and conformational properties of Aβ(1-16)

Comparison of the chemical shifts of pAβ(1-16) and the non-phosphorylated peptide²⁶ shows several signals perturbed by inclusion of the phosphate group (Table S1). Among them are Ser8 Hβs (Δδ ~ -0.20 and -0.24 ppm), His6 HN (Δδ ~ -0.22 ppm), Asp7 HN (Δδ ~ -0.13 ppm) and Ser8 HN (Δδ ~ -0.68 ppm). Such changes of the chemical shifts indicate the formation of hydrogen bonds between these amide protons and the phosphate group. The strongest interaction is between the phosphate group and the amide proton of the same residue, which leads to substantial low field shift of Ser8 HN. Interactions between the phosphate group and the backbone amide protons result in the packing of the central part of the peptide. Strong sequential HN-HN NOEs observed in the NOESY spectra of pAβ(1-16) (Fig. S1) indicate the formation of an α-helical fragment between residues 7 and 12. This distinguishes pAβ(1-16) from the unmodified human Aβ(1-16),²⁶ where the central part of the peptide is flexible and predominantly exists in an extended conformation.

Interaction of pAβ(1-16) with zinc ions alters the conformational state of the peptide: resonances from most of the residues 6-14 could not be detected in NMR spectra of pAβ(1-16) in the presence of Zn²⁺ (Table S1) due to significant line broadening of the signals. Such zinc-induced line broadening, typical for the Aβ fragments,²⁶⁻²⁸ has been found to be especially large in the case of pAβ(1-16) (Fig. S2). This indicates the existence of a complex conformational landscape of zinc-peptide bound states with more than one coordination site of the metal ion and several possible conformations of the complex.

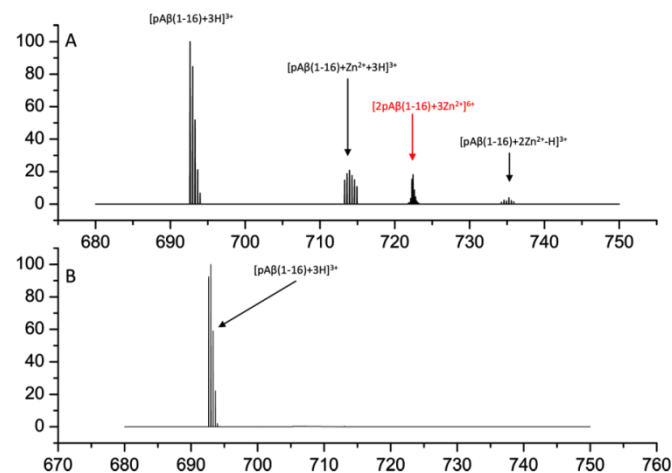


Fig. 2. The 670-760 m/z region of a mass-spectrum of pAβ(1-16) (10 μM) showing peptide monomers and formation or absence of dimer complexes in the presence (A) or absence (B) of zinc ions (300 μM zinc acetate) in a water-methanol (1:1) mixture, pH 7.3. Dimer complex with three zinc ions is shown in red.

Stoichiometry of the pAβ(1-16) interaction with zinc ions

The two-phase shape of the isotherm of pAβ(1-16) binding with zinc ions in the ITC experiments indicates that there are more than one Zn²⁺ binding site (Fig. 1). Indeed, this isotherm can be well fitted using the model of two independent binding sites (Table 1, Fig. 1).

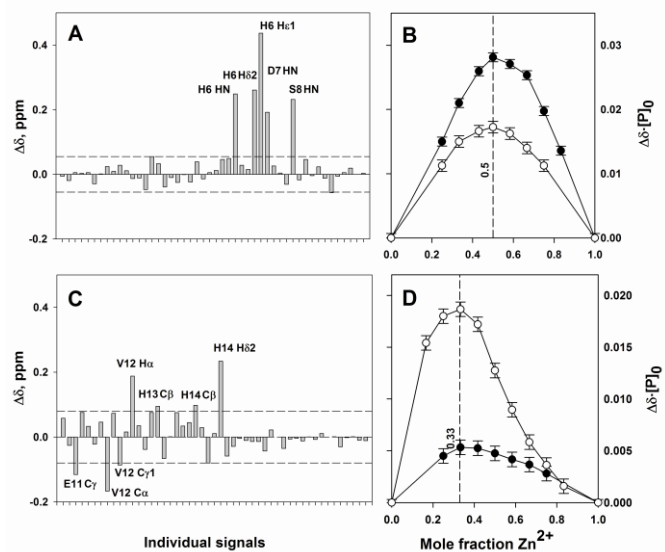


Fig. 3. Chemical shift changes of the individual signals of 0.5 mM pA β (1-10) (A) and 0.5 mM A β (11-16) (C) caused by the presence of 10-fold molar excess of Zn $^{2+}$. Changes in ^{13}C chemical shifts were normalized by a factor of 0.1 for adequate comparison with the ^1H data. Results of Zn $^{2+}$ isomolar titration of the fragments pA β (1-10) (B) and A β (11-16) (D). Abscissa represents the mole fraction of ZnCl $_2$, and the ordinate axis shows the product of $\Delta\delta\cdot[\text{P}]_0$, where $\Delta\delta$ - chemical shift change and $[\text{P}]_0$ - total peptide concentration in the sample. Reference lines (dotted) drawn at 0.5 and 0.33 correspond to 1:1 and 2:1 stoichiometry of binding. (B): Closed circles correspond to changes of the chemical shift of Ser8 HN signal at total concentration of [peptide] + [zinc] of 0.5 mM; open circles relate to chemical shift changes of Phe4 H δ^* at total concentration of 0.05 mM. (D): Closed triangles correspond to changes of the chemical shift of His14 H β 1 at total concentration of [peptide] + [zinc] of 0.5 mM; open triangles represent chemical shift changes of His14 H ϵ 1 at total concentration of 5 mM. Experiments were carried out in 10 mM Bis-Tris- d_{19} , in 90% H $_2\text{O}$ /10% D $_2\text{O}$, pH 6.9 (A-C) or in D $_2\text{O}$, pD 7.2 (D).

Thermodynamic parameters of zinc ions binding indicate as favorable only the entropic contribution to binding for both sites (Table 1). This is the essential difference between zinc binding by pA β (1-16) and A β (1-16) (Table 1). The large positive entropy of Zn $^{2+}$ binding to pA β (1-16) points at a significant reduction of hydrophobic surface exposed to solution, 29 which in turn indicates a more compact structure of this complex in comparison with A β (1-16). Stoichiometry of Zn $^{2+}$ binding to the high-affinity site of pA β (1-16) is close to 1, while stoichiometry of Zn $^{2+}$ binding to the low-affinity site is equal to 0.5 (Table 1), indicating dimer formation. Thus, the total amount of zinc ions per pA β (1-16) dimer is equal to three, with dimerization occurring through one zinc ion, while the other two zinc ions bind to the new sites of both subunits.

ESI-MS was used to verify the stoichiometry obtained by ITC. The pA β (1-16) dimer with three Zn $^{2+}$ ions was observed (Fig. 2, red) while in the absence of zinc ions no dimeric species of pA β (1-16) were detected (Fig. 2). This is in good agreement with the ITC data.

Localization of zinc ions binding sites in pA β (1-16)

To localize zinc ions binding sites for pA β (1-16) in the ITC experiments, a set of fragments and alanine mutants of this peptide has been used (Table 1). It was shown previously that A β (1-16) with non-protected termini is poorly soluble at physiological pH in the presence of zinc ions. $^{30-32}$ In contrast, the peptide with the acetylated N-terminus and amidated C-terminus remains soluble upon addition

of zinc salts. 23,26,31 Accordingly we have used pA β (1-16) with protected termini to study its interaction with zinc ions. In order to rule out participation of the N-terminal amino and C-terminal carboxyl groups of the peptide pA β (1-16) in chelation of zinc ion, we have compared thermodynamic binding parameters of the pA β (1-16) peptides with protected and non-protected termini (Table 1). Both peptides equally bind Zn $^{2+}$, indicating that N- and C- termini of the pA β (1-16) are not participating in Zn $^{2+}$ binding. Previously, we have shown that fragment A β (11-14) not only plays an important role in the chelation of the zinc ion, 23 but also serves as an interface for zinc-induced dimerization of A β (1-16). 24 This leads to the suggestion that the same site participates in the dimerization of pA β (1-16). Indeed, the reduction of the pA β (1-16) by six amino acids at the C-terminus (pA β (1-16) \rightarrow pA β (1-10)) leads to the loss of the binding site with stoichiometry of 0.5, and the fragment A β (11-16) by contrast forms dimers when titrated by Zn $^{2+}$ (Table 1). Potential zinc ion chelators in the N-terminal part of pA β (1-16) are the residues Asp1, Glu3, His6, Asp7 and pSer8. ITC data show that replacing Asp1, Glu3, and Asp7 with alanine results only in minor changes of the thermodynamic parameters of zinc ions binding, indicating that these residues do not participate in its coordination. Also, titration of the fragments pA β (1-10)H6A and pA β (7-9) by Zn $^{2+}$ was not followed by the release of heat (Table 1). These data demonstrate that His6 and pSer8 are necessary for Zn $^{2+}$ coordination and that the fragment pA β (6-8) forms the second Zn $^{2+}$ binding site of pA β (1-16).

Zinc coordination sites in the fragments pA β (1-10) and A β (11-16) were unambiguously confirmed by NMR. Zn $^{2+}$ titration experiments carried out on pA β (1-10) (Fig. S3) showed that increased concentrations of zinc affected the chemical shifts of side chain resonances for only two residues - His6 and Ser8 (Fig. 3A). The imidazole ring of His6 and the Ser8 phosphate group provide three of the four zinc coordination bonds. The fourth chelator is a backbone carbonyl group of His6 or Asp7. Backbone amide resonances of His6, Asp7 and Ser8 experience substantial zinc-induced changes of the chemical shifts. Changes of Ser8 amide proton relate to the weakening of the strong intra-residue hydrogen bond with the phosphate group upon its coordination with the zinc ion. However changes in the chemical shifts of HNs of His6 and Asp7 indicate the participation of carbonyl oxygen atoms conjugated with corresponding amide protons in the coordination of Zn $^{2+}$.

Changes in the chemical shifts of Ser8 HN and F4 H δ^* were used to determine stoichiometry of interaction of pA β (1-10) with zinc ions at two peptide concentrations, and it is 1:1, as follows from the results of the isomolar titration (Fig. 3B). NMR Zn $^{2+}$ titration experiments carried out on the A β (11-16) fragment (Fig. S4) allowed to identify the residues Glu11 and His14, coordinating a single zinc ion. These two residues undergo the most significant zinc-induced chemical shift changes (Fig. 3C). The observed changes in the Val12 resonances reflect the conformational transition of the peptide molecule upon zinc binding. Isomolar titration experiments carried out on the A β (11-16) fragment using His14 H β 1 and H ϵ 1 resonances to monitor zinc binding (Fig. 3D) show that the stoichiometry of the peptide-zinc interaction is 2:1. Similarly to pA β (1-10) these experiments were carried out at two peptide concentrations. Obtained results confirm the formation of a peptide dimer where the $^{11}\text{EVHHQK}^{16}$ fragment interacts with the Zn $^{2+}$ ion. It should be noted that 10-fold changes in the peptide concentration did not alter the stoichiometry of zinc-peptide interaction as revealed by the isomolar titration experiments (Fig. 3B, D).

ARTICLE

Discussion

In this work, we have studied the impact of Ser8 phosphorylation on Zn^{2+} binding by $A\beta(1-16)$. We have established that the phosphorylation of Ser8 leads to dramatic conformational changes in the $A\beta$ metal-binding domain, and formation of a new Zn^{2+} binding site – ${}^6HDpS^8$, where the zinc ion is coordinated by the imidazole ring of His6, phosphate group attached to Ser8 and a backbone carbonyl group of His6 or Asp7. The ${}^{11}EVHH^{14}$ site forms

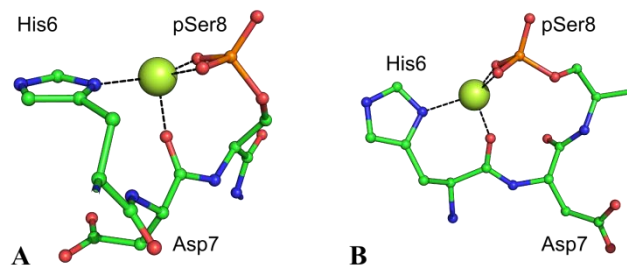


Fig. 4. Coordination modes of the zinc cation in $pA\beta(1-16)$ by the residues pSer8, Asp7, and His6 derived from QM/MM geometry optimization performed with GROMACS/CPMD.⁴⁴ (A) Zinc ion coordination involving oxygen from the main chain of Asp7. (B) Zinc ion coordination involving oxygen from the main chain of His6. Sphere indicates the zinc cation, amino acid residues in the peptides are shown in a ball-and-stick model.

the dimerization interface where the zinc ion is coordinated by the Glu11 and His14 residues of the two peptide subunits. The concentration of zinc ions may rise locally in the synaptic cleft up to a millimolar concentration (0.2–0.3 mM),^{33,34} specifically in the areas of amyloid peptides localization.³⁵ Furthermore, when the peptides *in vivo* are positioned in the macromolecular environment, dimerization processes are entropically much more favorable than in our model studies. The review by Wärmländer et al. supports this showing that $Zn/A\beta$ interactions become substantially stronger upon self-aggregation of the peptide *in vivo*.³⁶ Thus, the observed values of K_a for Zn^{2+} ions interaction with $pA\beta(1-16)$ (Table 1) could be relevant *in vivo*.

To model putative structure of the novel zinc binding site ${}^6HDpS^8$, QM/MM simulations were performed similar to those described earlier for the complex of ${}^{11}EVHH^{14}$ fragment with a zinc ion.²⁴ Models of the two types of zinc coordination by the ${}^6HDpS^8$ site have been built. In the first model (Fig. 4A), the phosphate group provides two oxygen atoms for the zinc coordination, the third bond is formed by the N_δ atom of the His6 side chain, and the fourth coordinator is the carbonyl oxygen of Asp7. In the second model (Fig. 4B) all coordination partners are the same except for the carbonyl oxygen of Asp7, which is substituted by the carbonyl oxygen of His6. Quantum mechanics calculations (S7) have shown that the system energy values for the two examined modes of coordination are almost identical. The computed enthalpies of complex formation shown in Fig. 4 differ by no more than 6 kcal·mol⁻¹. The second model of coordination where the fourth chelator is represented by the backbone carbonyl oxygen of His6, is energetically more favorable. It appears highly probable that both of these forms exist in solution, which is also consistent with the NMR data.

Although $A\beta(1-16)$ is capable of forming dimers in the presence of zinc ions, in solution it predominantly exists in the monomeric form. We established previously that when a monomeric complex is formed, Zn^{2+} is initially recognized and captured by the ${}^{11}EVHH^{14}$ region, and then the His6 approaches the coordination

Molecular BioSystems

sphere of zinc and locks it.²³ Using surface plasmon resonance biosensing and ESI-MS we demonstrated that the same region, ${}^{11}EVHH^{14}$, forms the $A\beta(1-16)$ dimerization interface where the zinc ion is coordinated by the Glu11 and His14 of the two peptide subunits.²⁴ Thus, the key event leading to the $pA\beta(1-16)$ dimerization, is the “exclusion” of His6 from zinc chelation in conjunction with the ${}^{11}EVHH^{14}$ site, as shown in Fig. 5. Being involved in the formation of a new zinc binding site together with pSer8, His6 loses its ability to complete the coordination sphere of zinc ion after its contact with the recognition site ${}^{11}EVHH^{14}$ of $pA\beta(1-16)$ (Fig. 5B). This leads to completing of the sphere by another $pA\beta(1-16)$ molecule, and consequently shifting of the thermodynamic equilibrium toward the formation of dimers. The proposed molecular mechanism of zinc-induced dimerization could contribute to the understanding of the initiation process of pathological $A\beta$ aggregation.

Aberrant protein phosphorylation is one of the defining pathological hallmarks of different neurodegenerative disorders, including AD.^{37,38} Currently the role of tau hyper-phosphorylation in the AD onset is being actively studied,¹² but the significance of $A\beta$ phosphorylation is poorly understood. $pA\beta$ is detected in the neurons of mouse models of AD at early stages of the disease, and at the latter stages in the amyloid plaques.^{12,22} Unlike $A\beta$, which is detected in neurons in the monomeric form, $pA\beta$ was found mainly in the form of dimers and oligomeric assemblies.^{12,22} This is consistent with our results showing that phosphorylation of Ser8 leads to a shift in the equilibrium towards the formation of dimers. All these data suggest that disruption of the phosphorylation mechanisms is a critical event in the development of AD, leading to changes in the aggregation properties of proteins implicated in the AD pathogenesis.

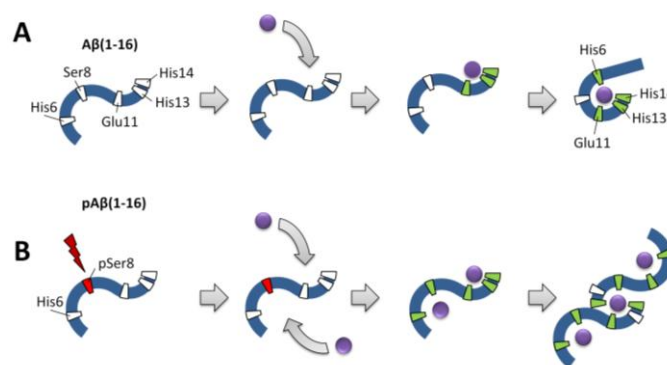


Fig. 5. Schematic diagram representing the Zn^{2+} interaction with $A\beta(1-16)$ (A) and zinc-induced dimerization of $pA\beta(1-16)$ (B). Peptides are shown in blue, zinc ions in violet, pSer8 not bound with zinc is shown in red and residues which coordinate zinc ions in green. (A) At the first step the zinc ion binds with the primary recognition site ${}^{11}EVHH^{14}$ of $A\beta(1-16)$ and then His6 closes the coordination sphere of zinc.²³ (B) pSer8 and His6 form the new zinc binding site of $pA\beta(1-16)$. As a result His6 cannot close the coordination sphere of zinc ion leading to dimer formation.

Experimental

Materials

All chemicals and solvents were of HPLC-grade or better and were obtained from Sigma-Aldrich (USA). All synthetic peptides (purity > 98%, checked by RP-HPLC) were purchased from Biopeptide Co., LLC (USA). The N- and C-termini of each peptide were protected with acetyl and amide, respectively; peptides pA β (1-16)open, pA β (7-9), pA β (6-9), and A β (11-16) were not protected at the N- and C-termini. The amino acid sequence of each peptide was confirmed on an ultra high resolution Fourier transform ion cyclotron resonance mass-spectrometer Bruker 7T Apex-Qe (Bruker Daltonics, USA) using a de-novo sequencing approach based on collision induced dissociation (CID) fragmentation. The lyophilized peptides were dissolved in buffer before each experiment. The final peptide concentrations were determined by UV absorption spectroscopy using the extinction coefficient of 1450 M⁻¹ cm⁻¹ at 276 nm (from Tyr 10 of A β) or gravimetrically.

Isothermal Titration Calorimetry

The thermodynamic parameters of zinc binding to pA β (1-16) fragments and mutants (Table 1) were measured using a MicroCal iTC200 System (GE Healthcare Life Sciences, USA) as described previously.³⁹ Experiments were carried out at 25°C in 20 mM Pipes buffer in the presence of 160 mM NaCl, pH 7.3. 2- μ l aliquots of the ZnCl₂ solution were injected into the 0.2 ml cell containing the peptide solution to obtain a complete binding isotherm. Peptide concentration in the cell ranged from 0.1 to 0.5 mM and ZnCl₂ concentration in the syringe ranged from 1 to 5 mM. The heat of dilution was measured by injecting the ligand into the buffer solution; the values obtained were subtracted from the heat of reaction in order to obtain the effective heat of binding. The resulting titration curves were fitted using MicroCal Origin software. Affinity constants (K_a), binding stoichiometry (N) and enthalpy (Δ H) were determined by a non-linear regression fitting procedure.

NMR spectroscopy

Peptide samples of 0.2 – 2.2 mM pA β (1-16), 0.05 – 4.0 mM pA β (1-10) and 0.05 – 8.0 mM A β (11-16) for NMR measurements were prepared in 10 mM solution of bis-Tris-d₁₉ (2,2-Bis(hydroxymethyl)-2,2',2''-nitrilotriethanol-d₁₉) with 98% ²D enrichment. Sodium salt of 3-(trimethylsilyl)propionic-2,2,3,3-d₄ acid in the concentration of 35 μ M was added as a standard in all NMR samples. To avoid pH variation in zinc titration experiments, both peptide and ZnCl₂ were dissolved in 10 mM bis-Tris-d₁₉ solution with identical pH from 6.80 to 6.95 measured in H₂O or identical pD from 7.20 to 7.40 measured in D₂O. NMR spectra were acquired at 283 K in 90% H₂O/10% D₂O on a Bruker AVANCE spectrometer operating at 600 MHz ¹H frequency (Bruker Daltonics, USA). 1D NMR spectra were processed by TopSpin 2.0 software. 2D NMR spectra were processed by NMRPipe⁴⁰ and analyzed using Sparky.⁴¹ The ¹H, ¹⁵N and ¹³C signal assignments of the peptides and their zinc complexes were obtained using the following 2D spectra: DQF-COSY, TOCSY (mixing time of 70 ms), NOESY (mixing time 200 ms), ROESY (mixing time 150 and 300 ms), ¹³C-¹H HSQC and ¹⁵N-¹H HSQC. Heteronuclear experiments were acquired at natural abundance of ¹³C and ¹⁵N isotopes. Method of continuous variations⁴² was used to determine stoichiometry of zinc binding to

pA β (1-10) and A β (11-16) peptides. This involved preparation of a series of samples containing both peptide and ZnCl₂ in varying proportions of the components, but in a fixed total concentration. Total concentration of [peptide] + [zinc] was kept at 0.05 or 0.5 mM for pA β (1-10), and 0.5 or 5.0 mM for A β (11-16). Changes of the chemical shifts induced by the interaction with zinc ions were subsequently analyzed. The plot of the product $\Delta\delta \cdot [P]_0$ ($\Delta\delta$ - change of the chemical shift; [P]₀ - total peptide concentration in the sample) versus the mole fraction of ZnCl₂ shows maximum at the fraction value, which corresponds to the stoichiometry.⁴²

Mass spectrometry

All experiments were carried out on a 7T Thermo Finnigan LTQ FT Ultra mass spectrometer (Germany) with electrospray ionization (ESI). The pA β (1-16) peptide was dissolved in a water-methanol (1:1) mixture, pH 7.3, with zinc acetate as the source for zinc ions. The solution composition, temperature of heated capillary, voltage, distance between the electrospray needle and the heated capillary inlet were varied in order to optimize the ionization conditions since formation of the metal-peptide complex is favored in basic solutions while ESI requires more acidic conditions. Peptide concentration in the solution varied from 200 nM to 10 μ M, and the concentration of zinc ions from 200 nM to 2 mM. The whole range of Zn²⁺/peptide ratio was explored (from 1:1 to 10:1 for [pA β (1-16)]/[Zn²⁺] ratio and from 1:1 to 10000:1 for [Zn²⁺]/[pA β (1-16)] ratio) in order to optimize the experimental conditions. The concentrations of the analyzed compounds were selected (10 μ M pA β (1-16) and 300 μ M Zn²⁺), that ensured stable and reproducible spectra. The analysis was performed using Thermo Finnigan QualBrowser.

Quantum-mechanics/molecular-mechanics calculations

The model of the structure of the A β (11-14) complex with zinc ion described earlier²⁴ was used to build a model of the complex consisting of the two chains of pA β (1-16) with three Zn²⁺ ions, using the PyMol program.⁴³ The molecular mechanics model of this structure was parameterized using the parm99sb force field. The model contained parameters corresponding to the geometry of the complex in which the zinc atoms are coordinated by the Glu11 and His14 residues of the two peptides, and the pSer8 and His6 from each peptide chain. Further model optimization and implicit solvent sampling simulations were done as described earlier for the 2A β (11-14)-Zn²⁺ complex.²⁴ The detailed procedure of QM/MM calculations is described in Supplementary data (S7).

Conclusions

It has been found that phosphorylation at Ser8 substantially changes the conformation, zinc-binding properties of the metal-binding domain of A β and favors its dimerization. Segment ⁶HDpS⁸ forms a novel zinc-binding site. Its interaction with zinc ions alters the metal-peptide equilibrium and induces formation of the dimers via the ¹¹EVHH¹⁴ site formed by the two pA β (1-16) chains. Together with the previous findings²⁴ these data support our hypothesis^{23,24} arguing the importance of ¹¹EVHH¹⁴ region in Zn²⁺-induced dimerization of A β . These results allow to consider this tetrapeptide as a promising drug target for the prevention of amyloidogenesis.

Acknowledgements

This work was supported by the Molecular and Cellular Biology and Fundamental Sciences to Medicine Programs of

ARTICLE

the Russian Academy of Sciences, by the Russian Foundation for Basic Research (grants 13-04-40108-comfi, 12-04-31925-mol_a), and by the Ministry of Education and Science of the Russian Federation (agreement №14.Z50.31.0014, agreement №14.BBB.21.0193, ID RFMEFI--14X0089). The supercomputer SKIF Chebyshev of M.V. Lomonosov Moscow State University was used for calculations.

Notes and references

^a Engelhardt Institute of Molecular Biology, Russian Academy of Sciences, Vavilov street 32, 119991 Moscow, Russia.

*E.mail: aamakarov@eimb.ru

^b Emanuel Institute of Biochemical Physics, Russian Academy of Sciences, Kosygina street 4, 119334 Moscow, Russia.

^c Faculty of Fundamental Medicine, M.V. Lomonosov Moscow State University, Lomonosovski prospect 31/5, 119191 Moscow, Russia.

^d Bioengineering and Bioinformatics Department, M.V. Lomonosov Moscow State University, Leninskie Gory 1, 119991 Moscow, Russia.

^e Howard Hughes Medical Institute, New York University School of Medicine, New York, 10016 New York, USA.

^f Orekhovich Institute of Biomedical Chemistry, Russian Academy of Medical Sciences, Pogodinskaya street 10, 119832 Moscow, Russia.

† Electronic Supplementary Information (ESI) available: Methods, Fig. S1-S4, Table S1. See DOI: 10.1039/b000000x/

1. J. Hardy, *J. Alzheimers Dis.*, 2006, **9**, 151-153.
2. J. A. Hardy and G. A. Higgins, *Science*, 1992, **256**, 184-185.
3. A. I. Bush, W. H. Pettingell, Jr., M. de Paradis, R. E. Tanzi and W. Wasco, *J Biol Chem*, 1994, **269**, 26618-26621.
4. M. A. Lovell, J. D. Robertson, W. J. Teesdale, J. L. Campbell and W. R. Markesbery, *J Neurol Sci*, 1998, **158**, 47-52.
5. M. Meyer-Luehmann, J. Coomaraswamy, T. Bolmont, S. Kaeser, C. Schaefer, E. Kilger, A. Neuenschwander, D. Abramowski, P. Frey, A. L. Jaton, J. M. Vigouret, P. Paganetti, D. M. Walsh, P. M. Mathews, J. Ghiso, M. Staufenbiel, L. C. Walker and M. Jucker, *Science*, 2006, **313**, 1781-1784.
6. F. Langer, Y. S. Eisele, S. K. Fritschi, M. Staufenbiel, L. C. Walker and M. Jucker, *J Neurosci*, 2011, **31**, 14488-14495.
7. N. G. Milton, *Neuroreport*, 2001, **12**, 3839-3844.
8. S. Schilling, U. Zeitschel, T. Hoffmann, U. Heiser, M. Francke, A. Kehlen, M. Holzer, B. Hutter-Paier, M. Prokesch, M. Windisch, W. Jagla, D. Schlenzig, C. Lindner, T. Rudolph, G. Reuter, H. Cynis, D. Montag, H. U. Demuth and S. Rossner, *Nat Med*, 2008, **14**, 1106-1111.
9. R. Shapira, G. E. Austin and S. S. Mirra, *J Neurochem*, 1988, **50**, 69-74.
10. T. C. Saido, W. Yamao-Harigaya, T. Iwatsubo and S. Kawashima, *Neurosci Lett*, 1996, **215**, 173-176.
11. A. E. Roher, K. C. Palmer, E. C. Yurewicz, M. J. Ball and B. D. Greenberg, *J Neurochem*, 1993, **61**, 1916-1926.
12. S. Kumar and J. Walter, *Aging (Albany NY)*, 2011, **3**, 803-812.
13. S. Fossati, K. Todd, K. Sotolongo, J. Ghiso and A. Rostagno, *Biochem J*, 2013, **456**, 347-360.
14. T. Shimizu, A. Watanabe, M. Ogawara, H. Mori and T. Shirasawa, *Arch Biochem Biophys*, 2000, **381**, 225-234.
15. F. Xin and P. Radivojac, *Bioinformatics*, 2012, **28**, 2905-2913.
16. D. J. Lee, D. L. Carlson, H. M. Lee, L. A. Ray and K. S. Markides, *Am J Public Health*, 1991, **81**, 1471-1474.
17. T. Tomiyama, S. Asano, Y. Furiya, T. Shirasawa, N. Endo and H. Mori, *J Biol Chem*, 1994, **269**, 10205-10208.
18. P. O. Tsvetkov, I. A. Popov, E. N. Nikolaev, A. I. Archakov, A. A. Makarov and S. A. Kozin, *ChemBioChem*, 2008, **9**, 1564-1567.
19. V. A. Mitkevich, I. Y. Petrushanko, Y. E. Yegorov, O. V. Simonenko, K. S. Vishnyakova, A. A. Kulikova, P. O. Tsvetkov, A. A. Makarov and S. A. Kozin, *Cell death & disease*, 2013, **4**, e939.
20. S. A. Kozin, I. B. Cheglakov, A. A. Ovsepyan, G. B. Telegin, P. O. Tsvetkov, A. V. Lisitsa and A. A. Makarov, *Neurotox Res*, 2013, **24**, 370-376.
21. S. Kumar, N. Rezaei-Ghaleh, D. Terwel, D. R. Thal, M. Richard, M. Hoch, J. M. Mc Donald, U. Wullner, K. Glebov, M. T. Heneka, D. M. Walsh, M. Zweckstetter and J. Walter, *Embo J*, 2011, **30**, 2255-2265.
22. S. Kumar, O. Wirths, S. Theil, J. Gerth, T. A. Bayer and J. Walter, *Acta Neuropathol*, 2013, **125**, 699-709.
23. P. O. Tsvetkov, A. A. Kulikova, A. V. Golovin, Y. V. Tkachev, A. I. Archakov, S. A. Kozin and A. A. Makarov, *Biophys J*, 2010, **99**, L84-86.
24. S. A. Kozin, Y. V. Mezentsev, A. A. Kulikova, M. I. Indeykina, A. V. Golovin, A. S. Ivanov, P. O. Tsvetkov and A. A. Makarov, *Mol. BioSyst.*, 2011, **7**, 1053-1055.
25. C. L. Masters and D. J. Selkoe, *Cold Spring Harb Perspect Med*, 2012, **2**, a006262.
26. S. Zirah, S. A. Kozin, A. K. Mazur, A. Blond, M. Cheminant, I. Segalas-Milazzo, P. Debey and S. Rebuffat, *J Biol Chem*, 2006, **281**, 2151-2161.
27. A. N. Istrate, P. O. Tsvetkov, A. B. Mantsyzov, A. A. Kulikova, S. A. Kozin, A. A. Makarov and V. I. Polshakov, *Biophys J*, 2012, **102**, 136-143.
28. C. D. Syme and J. H. Viles, *Biochim Biophys Acta*, 2006, **1764**, 246-256.
29. I. Jelesarov and H. R. Bosshard, *J Mol Recognit*, 1999, **12**, 3-18.
30. C. A. Damante, K. Ösz, Z. n. Nagy, G. Pappalardo, G. Grasso, G. Impellizzeri, E. Rizzarelli and I. Sóvágó, *Inorganic Chemistry*, 2009, **48**, 10405-10415.
31. S. A. Kozin, S. Zirah, S. Rebuffat, G. H. Hoa and P. Debey, *Biochem Biophys Res Commun*, 2001, **285**, 959-964.
32. T. Miura, K. Suzuki, N. Kohata and H. Takeuchi, *Biochemistry*, 2000, **39**, 7024-7031.
33. S. Y. Assaf and S. H. Chung, *Nature*, 1984, **308**, 734-736.
34. L. Pan and J. C. Patterson, *PLoS ONE*, 2013, **8**, e70681.
35. C. J. Frederickson and A. I. Bush, *Biomaterials: an international journal on the role of metal ions in biology, biochemistry, and medicine*, 2001, **14**, 353-366.
36. S. Wärmländer, A. Tiiman, A. Abelein, J. Luo, J. Jarvet, K. L. Söderberg, J. Danielsson and A. Gräslund, *Chembiochem*, 2013, **14**, 1692-1704.
37. W. Noble, D. P. Hanger, C. C. Miller and S. Lovestone, *Front Neurol*, 2013, **4**, 83.
38. S. N. Thomas, D. Cripps and A. J. Yang, *Methods Mol Biol*, 2009, **566**, 109-121.

Molecular BioSystems

39. V. Haurlyliuk, V. A. Mitkevich, N. A. Eliseeva, I. Y. Petrushanko, M. Ehrenberg and A. A. Makarov, *Proc Natl Acad Sci U S A*, 2008, **105**, 15678-15683.
40. F. Delaglio, S. Grzesiek, G. W. Vuister, G. Zhu, J. Pfeifer and A. Bax, *Journal of biomolecular NMR*, 1995, **6**, 277-293.
41. T. D. Goddard and D. G. Kneller.
<http://www.cgl.ucsf.edu/home/sparky>.
42. L. Fielding, *Tetrahedron*, 2000, 6151-6170.
43. The PyMOL Molecular Graphics System, Version 1.5.0.4
Schrödinger, LLC.
44. P. K. Biswas and V. Gogonea, *J. Chem. Phys.*, 2005, **123**, 164114.